Towards understanding long offset moveout correction

John C. Bancroft

ABSTRACT

The behavior of data with long offset moveout correction can appear to be quite bizarre. This behavior is typically muted out when stacking CMP gathers. However, when using Kirchhoff migrations, it may not be evident and therefore included in the migration. I investigate the behavior of moveout, and moveout correction, for long offsets to understand the apparent movement of energy, especially in the presence of vertically varying velocities.

INTRODUCTION

Moveout correction (MOC) of data for constant velocity media is well understood. The moveout stretch is predictable and is a natural process that is "designed" to prevent aliasing of the data. MOC is typically applied to a CMP gather, but is also part of the migration process).

When velocities vary vertically, the resulting stretch can appear to be quite bizarre as the effect of velocity variation can produce much greater stretch than that expected with the constant velocities. This moveout stretched data is normally muted when stacking. However, the concepts of moveout correction also apply to Kirchhoff migration, and since migration uses longer offsets, this bizarre data may be included. Understanding the nature of moveout correction can therefore aid in improved imaging.

This paper uses a simple technique to visualize the effects of moveout correction in an ongoing study to gain insight to its behavior. I will assume that RMS velocities V are defined at T_0, and that ray times for the source T_s and receiver T_r are defined by the hyperbolic moveout equations,

$$T_s^2 = \frac{T_0^2}{4} + \frac{(x+h)^2}{V^2}, \quad \text{and} \quad T_r^2 = \frac{T_0^2}{4} + \frac{(x-h)^2}{V^2}, \tag{1}$$

where the scatterpoint is located at $x = 0$, the midpoint located at x, and the half-source-receiver offset is h. The above equations assume the sources located at $(x + h)$ and the receiver at $(x - h)$ as illustrated in Figure 1. This figure and equation (1) illustrate raypaths in the same plane typical of 2D data but can also apply to 3D data by vectorizing x and h. I will continue the 2D form for simplicity in the following discussion.

Normal moveout correction, stacking, and poststack migration, moves prestack energy to focus points. This movement of energy is really an approximation to summing prestack data that is define by the double-square-root (DSR) equation that combines the source and receiver ray traveltimes, i.e.,

$$T = t_s + t_r = \sqrt{\frac{T_0^2}{4} + \frac{(x+h)^2}{V^2}} + \sqrt{\frac{T_0^2}{4} + \frac{(x-h)^2}{V^2}}. \qquad (2)$$

In the prestack volume (x, h, t), the traveltime T defines a surface that is commonly referred to as Cheops pyramid and displayed in Figure 2. The DSR equation may also be expressed exactly as

$$T^2 = T_0^2 + \frac{4}{V^2}\left(x^2 + h^2 - \frac{4x^2h^2}{T^2V^2}\right). \qquad (2)$$

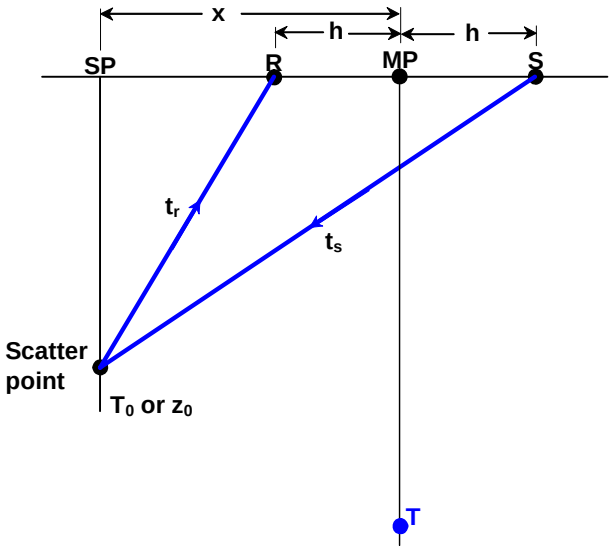

FIG. 1. Ray diagram for defining the double-square-root equation.

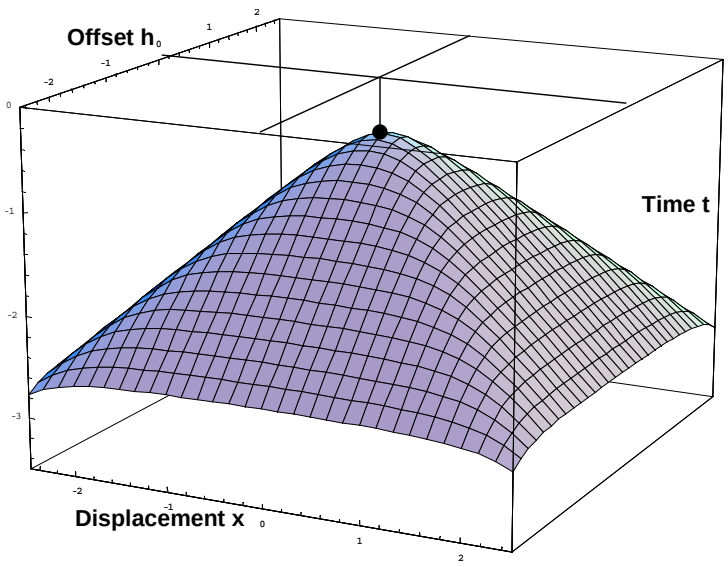

FIG. 2. The surface of the DSR equation defined in the prestack volume (*x*, *h*, *t*). This surface is referred to as Cheops pyramid.

Energy from the scatterpoint will be present in every prestack trace, provided the recording time is long enough. The energy from all these traces will lie on the surface defined by Cheops pyramid. It is the objective of prestack Kirchhoff migration (in fact all migrations) to move energy from every point on the surface back to the apex at a time T_0.

Similarly, moveout correction, stacking and poststack migration, attempt to achieve the same objective. The hyperbolic moveout moves energy in two time steps; from T to the moveout corrected time T_N, then from T_N to T_0 using poststack migration, i.e.

$$T^2 = T_N^2 + \frac{4h^2}{V^2} \quad \text{and} \quad T_N^2 = T_0^2 + \frac{4x^2}{V^2}, \tag{3}$$

as illustrated in Figure 3.

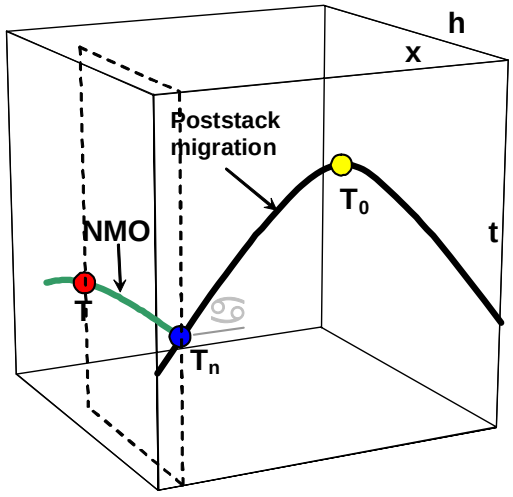

FIG. 3. Illustration to show that moveout correction and poststack migration is an approximation to the DSR assumption, and more specifically that moveout correction is part of the migration process.

Combining moveout correction and migration equations we get

$$T^2 = T_0^2 + \frac{4}{V^2}\left(x^2 + h^2\right). \tag{4}$$

Note the similarity to the exact equation (2), but more importantly the difference. One can improve the moveout equation by including a dip term (with dip β) i.e.,

$$T^2 = T_N^2 + \frac{4h^2\cos^2\beta}{V^2} = T_N^2 + \frac{4h^2\left(1-\sin^2\beta\right)}{V^2}, \tag{5}$$

to get

$$T^2 = T_0^2 + \frac{4}{V^2}\left(x^2 + h^2 - h^2 \sin^2 \beta\right). \qquad (6)$$

This equation is still not as precise as equation (2) and is often thought to be a definition of dip moveout (DMO). The main point is that moveout correction is part of the migration process.

MOVEOUT CONCEPTS

Rather than use wavelets, I will simplify the figures and use three lines with one that represent the center time, and the other two a delta time before and after the center time as illustrated in Figure 4. The outer lines could be assumed to represent the minima of a zero-phase wavelet. These delta times will be constant for data with moveout. Figure 4 represents a common midpoint (CMP) gather, or a common scatterpoint (CSP) using equivalent offset migration (EOM). The gather shows the three bundles of lines that represent three reflections, all with the same "wavelet".

Moveout correction is applied to the data in Figure 4 and displayed in Figure 5. Note the moveout stretch that is illustrated by the spreading of the outer lines on the three horizontal events. Muting would limit the offset to prevent data with too much stretch from entering the stack.

The model is now changed by using RMS velocities that increase linearly with time (not depth) and is shown in Figure 6. The velocity used in this example is $V_{rms} = 1000 + 1000T_0$, where T_0 is the time at zero offset. These velocities are quite low for real data, but are convenient for illustrating the moveout effects.

The shallow event at zero offset time T_0 = 0.2 sec. has the lowest velocity and has a greater moveout relative to the other events. The event at time T_0 = 1.0 sec. has the highest velocity and the flattest hyperbolic trajectory. These events intersect each other, creating difficulty for moveout correction.

Figure 7 shows the effect of moveout correction for each line in Figure 6. Note the extent of the moveout-stretch has increased and is due to the slight change in the velocity within the span of the wavelet. However, this moveout correction has only been applied locally to each event and has simplified the distribution of energy.

In Figure 6, the top two events cross the lower event at offsets 750 m and 1,000 m. During conventional MOC, energy from the lower event will also be moved to the two upper events. This effect is illustrated in Figure 8, which contains only the lower event. This figure also includes moveout trajectories at 0.1 sec. intervals. Energy at the location where these curves intersect the event is moveout corrected to the corresponding T_0, as identified by the coloured asterisks. The movement of the energy in Figure 8 is illustrated with a similar figure in Figure 9 in which the moveout trajectory at 0.5 sec. is highlighted with a red dashed curve to show its intersection with the event. Energy at the intersection is moveout corrected back to 0.5 sec., as illustrated with the red arrow.

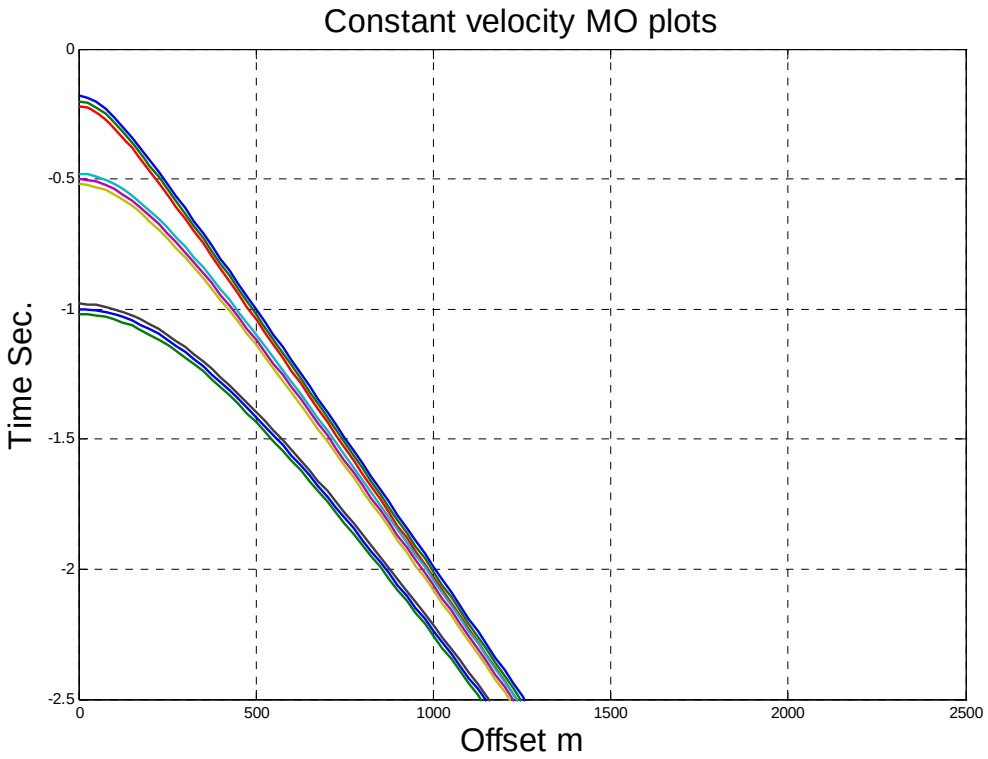

FIG. 4. Constant velocity hyperbolic moveout for three events, with lines representing the wavelet.

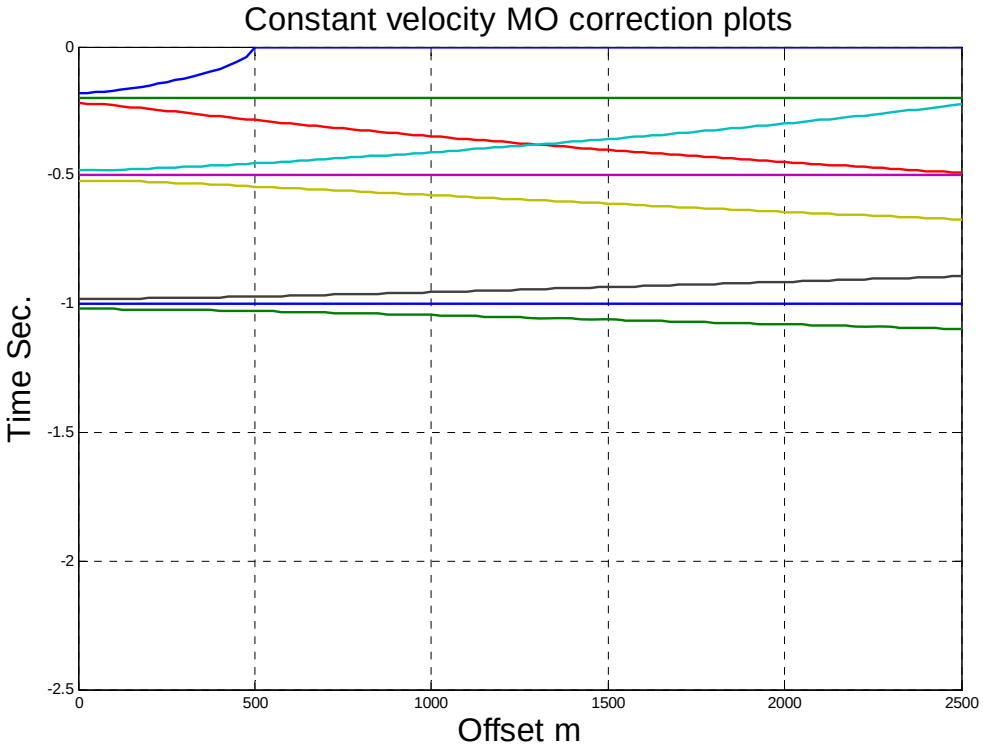

FIG. 5. Moveout correction applied to the data in Figure 4.

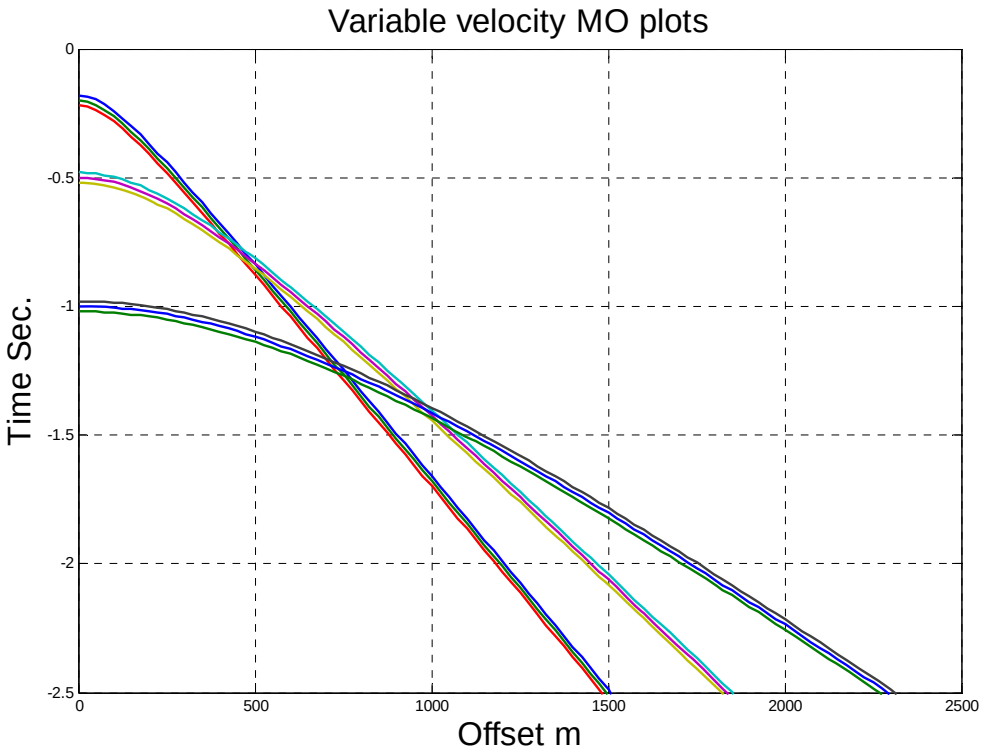

FIG. 6. Moveout for time-varying velocities

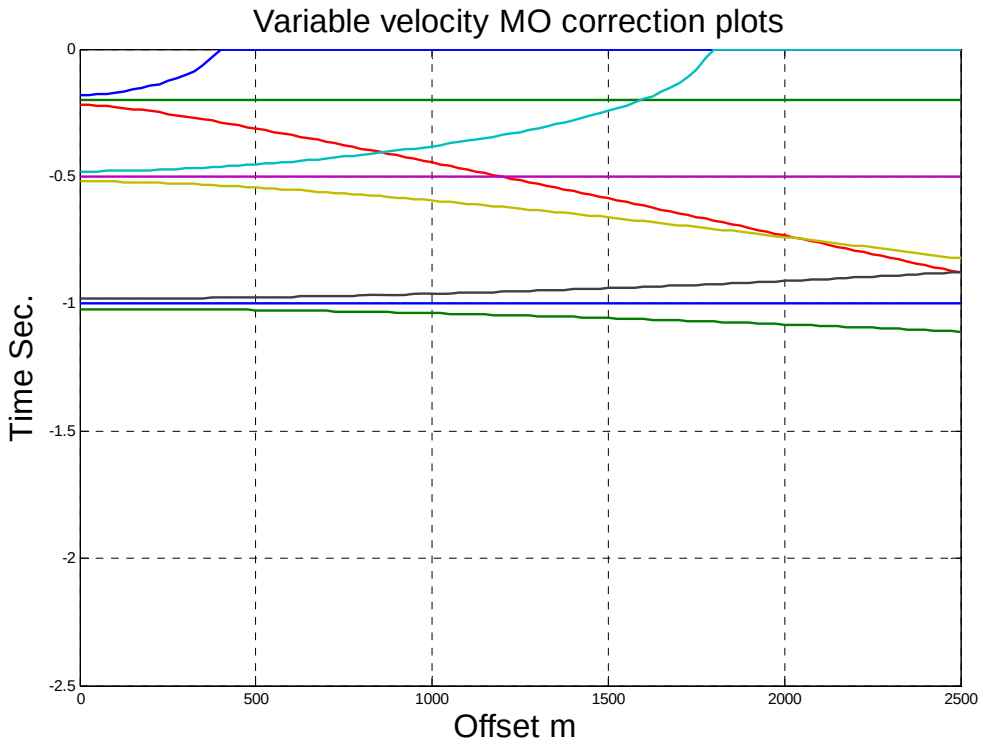

FIG. 7. Moveout correction applied to the data in Figure 6.

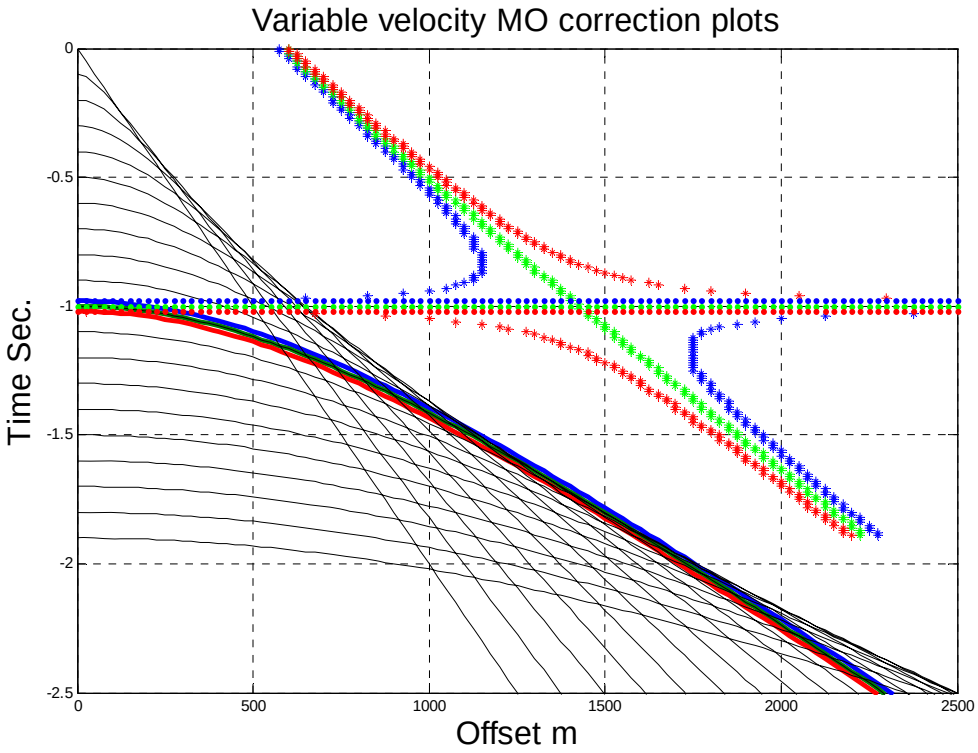

FIG. 8. Moveout correction of the event at 1.0 sec, which now uses moveout trajectories.

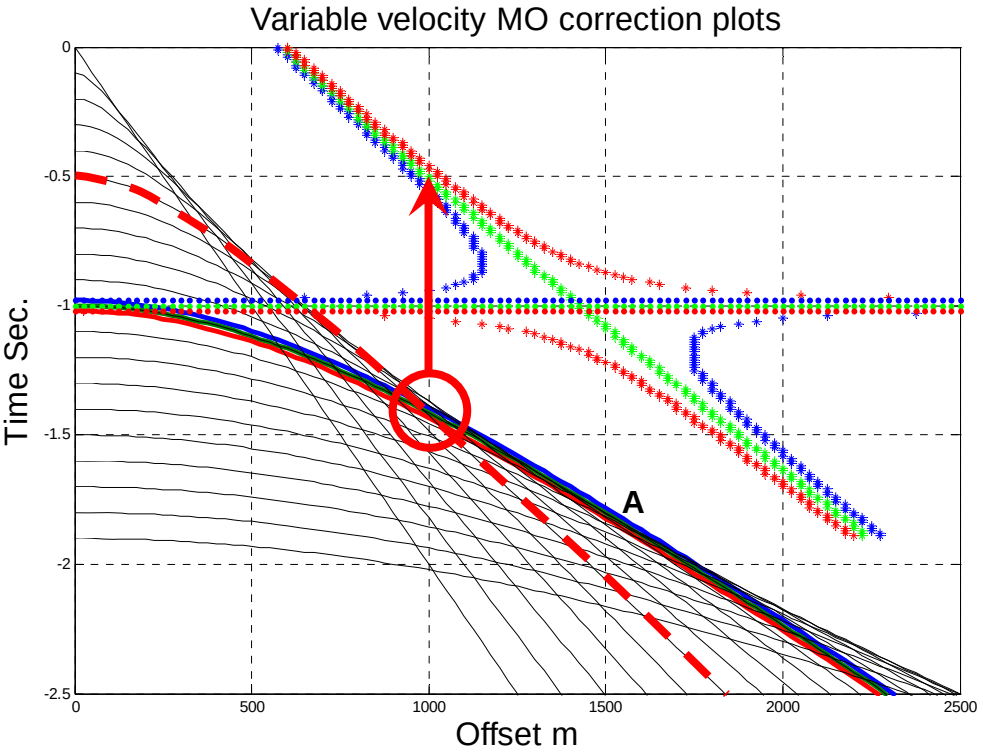

FIG. 9. Same as Figure 8, but the moveout trajectory from 0.5 sec. is highlighted in a dashed red to identify its intersection with the 1.0 sec. event.

The asterisks in Figures 8 and 9 illustrate the extent of relocated energy by moveout correction for just this single event. Energy at the 1,000 m offset will be spread between the two blue asterisks and the phase of the "wavelet" at t = 0.5 is inverted. Also note the change in the phase of the wavelet along t = 1.0 sec. and beyond 1,000 m offset. Although this smearing of data is typically muted out from the CMP gathers of real data, it can be viewed on prestack migrations of source gathers (shot records) and it could be included in the migrated image.

Let me again point out the simplicity of this model but the complexity of the results. These effects are often attributed to anisotropy and possibly interfere with amplitude verse offset (AVO) processing.

APPLYING MOVEOUT CORRECTION

The previous figures illustrate that reflection energy on a single seismic trace is multi-valued. A single point on a trace could be moved to at least two T_0 times with two different velocities defined by T_0, i.e., $V_{RMS}(T_0)$. This is not a problem in conventional processing for poststack migration as the data in a CMP gather, as it is moveout corrected using trajectories with velocities defined at zero offset with T_0 times.

In prestack migrations, the order in which data is summed over Cheops pyramid can be re-ordered to sum one complete input trace at a time into the migrated trace. Consider now the problem of applying moveout correction to one offset trace, at a random location, in the middle of a prestack migration. We know the velocity at the migrated location or zero offset, but this velocity is not defined at times on the offset trace. How do we find the velocity for the moveout correction? We don't know the T_0 yet, as that is what we are trying to find.

The forward problem for computing the moveout times is the hyperbolic equation

$$T^2 = T_0^2 + \frac{4h^2}{V_{rms}^2(T)_0}. \tag{7}$$

Now change the order of the equation to get the moveout corrected time T_0 as

$$T_0^2 = T^2 - \frac{4h^2}{V_{rms}^2(T_0)}. \tag{8}$$

That may look simple enough but note that we need the velocity that is defined at T_0, the time we are trying to find, and it is on the right side of the equation.

We get around this problem by using the forward equation (7), and start the process with T_0 = 0 on the migrated trace. Using this time, we get the velocity $V_{RMS}(T_0)$, compute T, then interpolate the data on the input trace and insert it into the migrated trace at T_0. We then go to the next migrated sample at T_0 = *delt*, then T_0 = *2delt* etc. As a consequence of this process, we get the smear of the third event in the above examples at shallower and deeper times as illustrated in Figure 10.

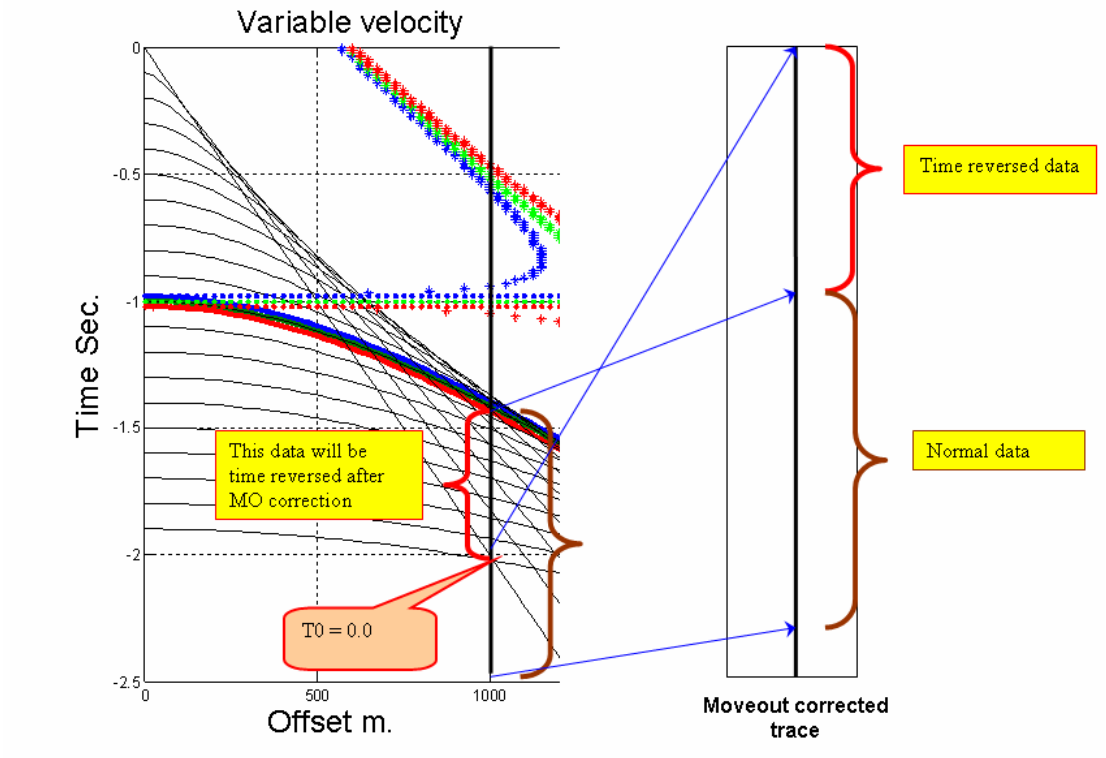

FIG. 10. Illustration of moveout correction for a single trace.

ALTERNATIVES TO MOVEOUT CORRECTION

A more correct process would be to perform a downward continuation process on a CMP or CSP gather that would unravel the overlapped energy and prevent the smearing. I believe that this is a significant benefit of prestack migration of source records that use wave propagation techniques.

Another alternative to conventional moveout is to use the high resolution radon transform. One form of it is used in the semblance plot to estimate the velocities, but it could also be used to produce a migrated trace with much of the "noise" removed, i.e., multiples, mode converted waves, etc.

THREE DIMENSIONAL VIEW OF THE MOVEOUT TRAJECTORIES

I will continue my investigation of moveout correction by revisiting Figure 9 in the area around offset 1500 m and time 1.75 sec., as identified the "**A**". This area contains an envelope of many trajectories that overlap. This data is viewed as a CMP or CSP gather on a two dimensional plane of offset and time (h, t). We could add another dimension to this data by including the zero-offset time "t_0", i.e., (h, t_0, t). Various 3D perspective views of the moveout curves, defined above are displayed in Figure 11.

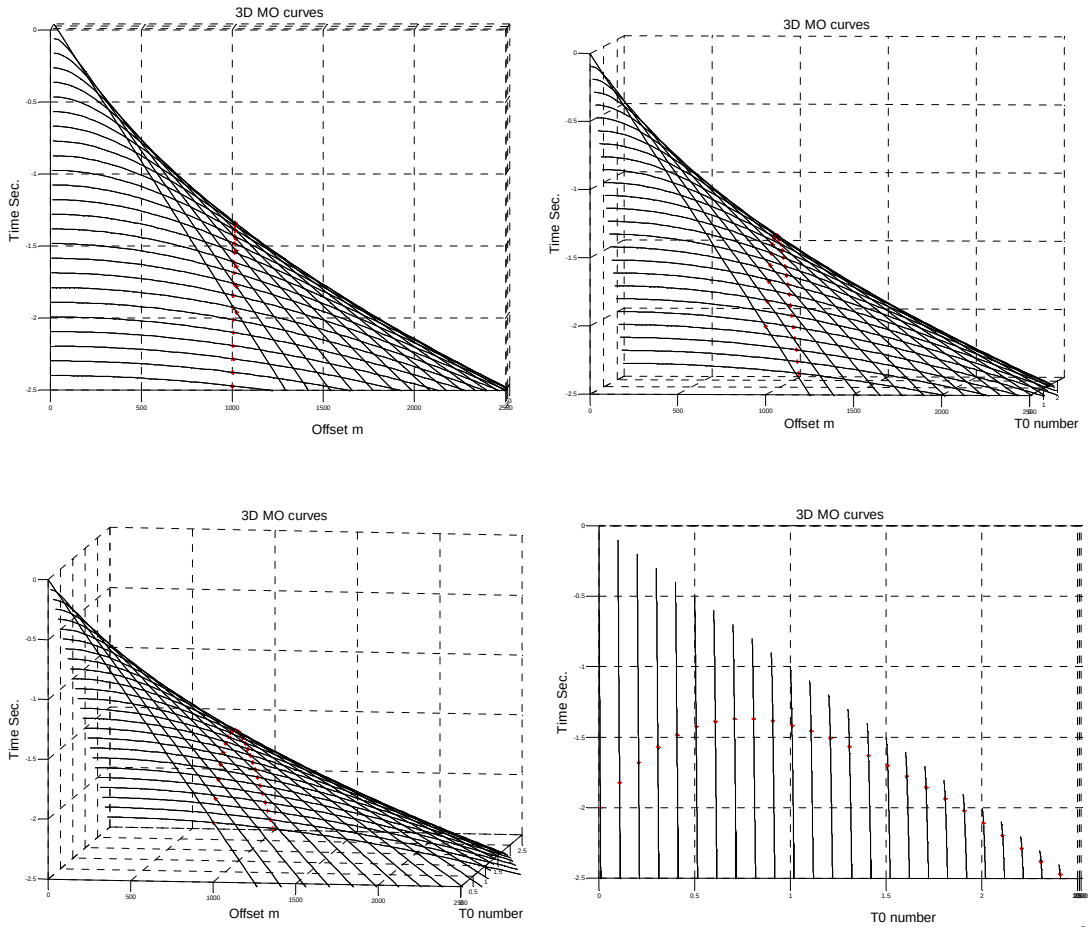

FIG. 11. Various 3D views of the CMP or CSP volume (h, T_0, t).

Each of the views in Figure 11 contains a red point that is defined at offset 1000 m on each trajectory. Those points that are normally smeared on the 2D examples are now separated. These times, at 1,000 m offset are now plotted in Figure 12 with axis of time $T_{1,000}$ and T_0.

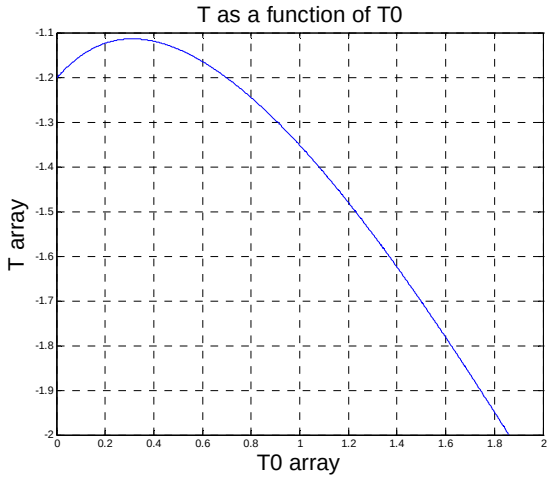

FIG. 12. Trajectory times T at offset h = 1,000 m verse zero-offset time T_0.

COMMENTS

I propose to apply moveout correction to CMP or CSP gathers in the 3D space (h, t_0, t) with constant velocities at each T_0. Only bands of moveout correction need to be applied around T_0 with a width that is about the size of a wavelet. Using this approach, I hope to be able to reduce the variable-velocity smear, improve AVO response, use longer offset, and achieve better imaging.

CONCLUSIONS

The effects of moveout correction are investigated with the intent of improving the images associated with prestack migration. The kinematic steps of moveout correction, stacking, and poststack migration, were compare to those of prestack Kirchhoff migration, to illustrate that moveout correction is part of the migration process. Data in a CMP or CSP gather that are normally displayed in a 2D image ((h, t) were displayed in a 3D volume by including an axis of T_0, i.e., (h, T_0, t). It is anticipated that this 3D volume may help reduce the smear caused by conventional moveout correction.

ACKNOWLEDGEMENTS

We are grateful for the financial support of the CREWES sponsors.